


Emergent power-law interactions in near-crystalline membranesPappu Acharya,^{*} Debankur Das,[†] Surajit Sengupta, and Kabir Ramola[‡]*Centre for Interdisciplinary Sciences, Tata Institute of Fundamental Research, Hyderabad 500107, India* (Received 2 November 2021; revised 24 March 2022; accepted 29 October 2022; published 28 November 2022)

We derive exact results for the fluctuations in energy produced by microscopic disorder in near-crystalline athermal systems. Our formalism captures the heterogeneity in the elastic energy of polydisperse soft disks in energy-minimized configurations. We use this to predict the distribution of interaction energy between two defects in a disordered background. We show that this interaction energy displays a disorder-averaged power-law behavior $\langle \delta E \rangle \sim \Delta^{-4}$ at large distances Δ between the defects. These interactions upon disorder average also display the sixfold symmetry of the underlying reference crystal. Additionally, we show that the fluctuations in the interaction energy encode the athermal correlations introduced by the disordered background. We verify our predictions with energy-minimized configurations of polydisperse soft disks in two dimensions.

DOI: [10.1103/PhysRevE.106.L052902](https://doi.org/10.1103/PhysRevE.106.L052902)

Introduction. Disordered amorphous materials exhibit heterogeneity in their elastic properties and arise in several physical as well as biological contexts. Examples include jammed systems and granular materials [1–4], densely packed tissues, cellular membranes [5–7], and systems displaying glassy behavior [8]. Such materials are classified as athermal, as they are only weakly affected by ambient thermal fluctuations, being governed at the local scale by the constraints of mechanical equilibrium [9–11]. These local constraints lead to randomness at the microscopic scale and thus disordered athermal systems are not described by the usual elasticity theories in continuum [12–14], instead exhibiting emergent elasticity properties upon disorder average [15]. Extending the techniques of continuum elasticity to include the presence of structural disorder, as well as developing a continuum theory describing the mechanics and elasticity of disordered amorphous solids, remains an outstanding challenge [14–20].

The dynamics of athermal systems is governed primarily by the motion in phase space through energy-minimized configurations and therefore characterizing their energy landscape is of central importance. Localized sources of stress play a key role in determining the energy density and also lead to heterogeneous elastic properties of amorphous materials. Interactions between stress defects in such systems involve the elasticity of the entire network [21], which is sensitively dependent on disorder. An average over disorder can lead to effective or emergent interactions that arise in many microscopic theories of matter [22–25]. Disordered athermal materials therefore provide an interesting arena where emergent interactions mediated by an elastic embedding material arise [26]. Characterizing the spatial distribution of the elastic energy as well as the fluctuations in the energy density produced by the underlying disorder is an important ingredient in any coarse-grained Hamiltonian-based elasticity theory.

Although continuum elasticity theories describe the behavior of systems at large length scales, they ignore the disorder present at the granular level. A microscopic derivation of interaction energies between defects is therefore useful in characterizing such energy landscapes that are also of fundamental importance in describing the dynamics of amorphous materials. However, the complexity of the energy landscape and the associated states of mechanical equilibrium makes such computations a challenging task.

In this context, near-crystalline jammed systems serve as extremely useful theoretical models with which to study the elasticity properties of disordered athermal materials. Near-crystalline jammed materials are often able to capture several nontrivial properties of amorphous solids [27–32] and provide a route towards a unified framework for crystalline and amorphous elasticity. For example, random spring networks have continued to serve as useful building blocks with which to understand such complex many-particle systems [33]. Lattice-based models of elasticity, consisting of a crystalline arrangements of soft particles, are also routinely employed to understand elasticity properties as well as their breakdown at the amorphous scale [28,34].

Several studies have sought to describe the interaction between defects within the framework of continuum elasticity [12,35–37], which displays a power-law behavior at large distances [21,38–45]. A crucial question therefore is whether such elastic interactions can emerge with the introduction of structural disorder in the system. However, despite the importance and several previous studies, an exact prediction of the energy of interaction between defects in disordered elastic materials at the grain level has not been reported. In this regard, exactly solvable models provide a fascinating arena to explore the short-length-scale physics of disordered materials. A prime candidate are near-crystalline jammed systems, where several exact predictions incorporating the effects of microscopic disorder can be made due to the simplicity of the contact network [29,46–49].

In this Letter we present exact results for the fluctuation in energy produced by microscopic disorder in near-crystalline

^{*}pappuacharya@tifrh.res.in[†]debankurd@tifrh.res.in[‡]kramola@tifrh.res.in

athermal systems. Our formalism predicts the *exact* energy of a system of soft disks with the quenched disorder in the particle sizes. Using this, we derive the *average* interaction energy between defects placed at different locations in a elastic membrane, which displays an emergent power-law behavior at large distances. We also predict the exact distribution of the energy of interaction between two defects in the polydisperse background. Our results demonstrate that fluctuations in the interaction energy between defects encode the effects of the athermal disorder in the polydisperse backgrounds, a feature absent in thermal fluctuations. Our theoretical results also provide insight into the orientation dependence of the interactions between elastic inclusions in near-crystalline systems.

Disordered athermal crystals. We study a system comprised of minimum-energy configurations of soft disks interacting through the well-studied one-sided potential [50,51]

$$U_{\sigma_{ij}}(\vec{r}_{ij}) = \begin{cases} \frac{K}{\alpha} \left(1 - \frac{|\vec{r}_{ij}|}{\sigma_{ij}}\right)^\alpha & \text{for } r_{ij} < \sigma_{ij} \\ 0 & \text{for } r_{ij} > \sigma_{ij}. \end{cases} \quad (1)$$

Here $\vec{r}_{ij} = \vec{r}_j - \vec{r}_i$ is the vector distance between the i th and j th particles located at positions \vec{r}_i and \vec{r}_j , respectively, and $\sigma_{ij} = \sigma_i + \sigma_j$ is the sum of their individual radii. We set the effective stiffness of the interactions to $K = 1$ for simplicity. Although our results are valid for general $\alpha > 1$, we present results for the harmonic case ($\alpha = 2$). Notably, the *disorder* in this pairwise interaction is encoded in the quenched radii $\{\sigma_i\}$. The interparticle forces are then given by $\vec{f}_{ij} = \frac{K}{\sigma_{ij}} \left(1 - \frac{|\vec{r}_{ij}|}{\sigma_{ij}}\right)^{\alpha-1} \hat{r}_{ij}$, where \hat{r}_{ij} is the unit vector in the \vec{r}_{ij} direction. We begin with a collection of equal-size soft disks with $\sigma_i = \sigma_0 = 1/2$. The minimum energy configuration is a crystalline state with the positions of the centers $\{\vec{r}_i^{(0)}\}$ forming a triangular lattice. The marginal crystal, with packing fraction $\phi_c = \pi/\sqrt{12} \approx 0.9069$, has no overlaps between particles and zero interparticle forces. We work with overcompressed configurations $\phi > \phi_c$ and the energy in the initial crystalline state $E_{ij}^{(0)}$ is equal at each bond ij . The total energy of the crystalline state is (see the Supplemental Material [52])

$$E^{(0)} = \frac{1}{2} \sum_{i=1}^N \sum_{j=0}^5 E_{ij}^{(0)} = \frac{3N}{2} \left(1 - \sqrt{\frac{\phi_c}{\phi}}\right)^2, \quad (2)$$

where N is the number of particles in the system. The superscript (0) denotes the crystalline state with equal-size particles. Next we introduce disorder in the system by varying the radii of the particles as

$$\sigma_i = (1 + \eta \xi_i) \sigma_0 = \sigma_0 + \delta \sigma_i. \quad (3)$$

Here ξ_i are independent and identically distributed random variables. We choose a uniform underlying distribution of $\xi_i \in [-\frac{1}{2}, \frac{1}{2}]$ [28]; however, our results are valid for any underlying distribution in the particle sizes. Our present work is focused on the regime of small polydispersity in the particle sizes, in which contacts between particles are rarely broken. Nevertheless, our predictions work fairly well in a regime where few contacts are broken (see the Supplemental Material [52]).

Exact displacement fields. We begin by deriving exact displacement fields in energy-minimized configurations with

small disorder in particle sizes. For each realization of the quenched disorder, the system is allowed to relax into an energy-minimized state, which is accomplished using the FIRE algorithm [53] in our numerical simulations. These configurations therefore satisfy the conditions of mechanical equilibrium, i.e., $\sum_j f_{ij}^x = 0$ and $\sum_j f_{ij}^y = 0$, for each particle at site $i \equiv \vec{r}$. Here $f_{ij}^{x(y)}$ are the $x(y)$ components of the interparticle force between particles i and j in contact. Therefore, in order to characterize the behavior of such a system, one needs to simultaneously solve *all* the force balance equations, which along with the force law yields a unique solution for particle displacements [29,46]. This can be accomplished with a systematic perturbation expansion about the crystalline ordered state, to linear order as well as higher orders [29,46,47]. When disorder is introduced into the system, the positions of the particles deviate from their crystalline values $\{\vec{r}_i^{(0)}\} = \{x_i^{(0)}, y_i^{(0)}\}$ to a new mechanical equilibrium configuration $\{\vec{r}_i^{(0)} + \delta \vec{r}_i\} = \{x_i^{(0)} + \delta x_i, y_i^{(0)} + \delta y_i\}$. The displacements can be expressed as a formal expansion

$$\delta \vec{r}_i = \delta \vec{r}_i^{(1)} + \delta \vec{r}_i^{(2)} + \delta \vec{r}_i^{(3)} + \dots, \quad (4)$$

where $\{\delta \vec{r}_i^{(n)}\} = \{\delta x_i^{(n)}, \delta y_i^{(n)}\}$ represent the n th-order displacement fields of magnitude $O(\eta^n)$. We focus on the terms up to second order $\delta x_i = \delta x_i^{(1)} + \delta x_i^{(2)}$ and $\delta y_i = \delta y_i^{(1)} + \delta y_i^{(2)}$, which contribute to the leading-order terms in the energy of the system. As the coefficients in the perturbation expansion are drawn from the underlying crystalline arrangement, the force balance equations can be solved hierarchically in Fourier space to obtain the displacement fields at every order [29]. The incremental radii $\{\delta \sigma\}$ and the lower-order displacement fields act as sources that generate the displacement fields at higher orders. At linear order, the displacements in Fourier space as a response to the disorder $\{\delta \sigma_i\}$ can be expressed as $\delta \vec{r}^{\mu \cdot (1)}(\vec{k}) = \tilde{G}^\mu(\vec{k}) \delta \sigma(\vec{k})$ [29]. Here $\delta \sigma(\vec{k}) = \sum_{\vec{r}} e^{i\vec{k} \cdot \vec{r}} \delta \sigma(\vec{r})$, δr^μ refers to δx and δy for $\mu = x, y$, respectively, and $\tilde{G}^\mu(\vec{k})$ represent the response Green's functions in Fourier space. The reciprocal lattice vectors for the triangular lattice arrangement are $\vec{k} \equiv (k_x, k_y) \equiv \left(\frac{2\pi l}{2L}, \frac{2\pi m}{L}\right)$ [54].

Energy of a disordered configuration. Importantly, the exact displacement fields can be used to compute the excess energy produced by an arbitrary configuration of excess radii over the crystalline background. The energy $E_{ij} = U(\vec{r}_{ij})$ of each bond ij can be expressed as a perturbation expansion in the displacement fields as

$$E_{ij} = E_{ij}^{(0)} + \sum_{\mu} e_{ij}^{\mu} \delta r_{ij}^{\mu} + \sum_{\mu} \sum_{\nu} e_{ij}^{\mu\nu} \delta r_{ij}^{\mu} \delta r_{ij}^{\nu} + e_{ij}^{\sigma} \delta \sigma_{ij} + e_{ij}^{\sigma\sigma} \delta \sigma_{ij} \delta \sigma_{ij}, \quad (5)$$

where the indices $\mu, \nu \equiv x, y$, and $\delta x(y)_{ij} = \delta x(y)_j - \delta x(y)_i$ represent the relative displacement fields up to all orders. The coefficients e_{ij}^{μ} and $e_{ij}^{\mu\nu}$ can be expressed purely in terms of the reference crystalline structure and are therefore translationally invariant, i.e., they do not depend on the site index i . Here $E_{ij}^{(0)}$ represents the energy of each bond ij in a pure crystal with no polydispersity in particle sizes. As the excess energy of the system incorporates second-order terms, we group terms in Eq. (5) that contribute up to second order. The excess energy of each bond above the crystalline value can then be expressed

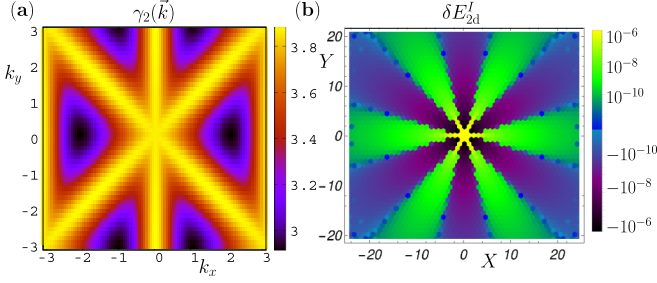


FIG. 1. (a) Plot of the interaction kernel $\gamma_2(\vec{k})$ in Fourier space, displaying the underlying crystalline symmetries. (b) Average energy of interaction between defects placed a distance $\vec{\Delta} \equiv (X, Y)$ apart. The average interaction energy displays positive and negative regions, reflecting the underlying crystalline background.

to leading order as $\delta E_{ij} = E_{ij} - E_{ij}^{(0)} = T_{1,ij}^{(1)} + T_{1,ij}^{(2)} + T_{2,ij}^{(1)}$. We have explicitly

$$\begin{aligned} T_{1,ij}^{(1)} &= e_{ij}^x \delta x_{ij}^{(1)} + e_{ij}^y \delta y_{ij}^{(1)} + e_{ij}^\sigma \delta \sigma_{ij}, \\ T_{1,ij}^{(2)} &= e_{ij}^x \delta x_{ij}^{(2)} + e_{ij}^y \delta y_{ij}^{(2)}, \\ T_{2,ij}^{(1)} &= e_{ij}^{xx} \delta x_{ij}^{(1)} \delta x_{ij}^{(1)} + e_{ij}^{xy} \delta x_{ij}^{(1)} \delta y_{ij}^{(1)} + e_{ij}^{yy} \delta y_{ij}^{(1)} \delta y_{ij}^{(1)} \\ &\quad + e_{ij}^{x\sigma} \delta x_{ij}^{(1)} \delta \sigma_{ij} + e_{ij}^{y\sigma} \delta y_{ij}^{(1)} \delta \sigma_{ij} + e_{ij}^{\sigma\sigma} \delta \sigma_{ij} \delta \sigma_{ij}, \end{aligned} \quad (6)$$

where the superscripts of T represent the order of the displacement field solution contributing to the energy and subscripts represent the order of the energy expansion. For example, $T_{2,ij}^{(1)}$ represents the second-order term in the energy expansion using the linear-order solution to the displacement fields. These terms are easily summed by taking Fourier transforms of the relevant fields. Interestingly, the contribution from the term containing the second-order displacement fields is precisely zero, i.e., $\sum_{ij} T_{1,ij}^{(2)} = 0$ (see the Supplemental Material [52]). The contributions from the other terms are

$$\sum_{ij} T_{1,ij}^{(1)} = \gamma_1 \delta \bar{\sigma}(0), \quad \sum_{ij} T_{2,ij}^{(1)} = \sum_{\vec{k}} \gamma_2(\vec{k}) \delta \bar{\sigma}(\vec{k}) \delta \bar{\sigma}(-\vec{k}), \quad (7)$$

respectively, where $\gamma_1 = \sum_j 2e_{ij}^\sigma$ and the exact expression for the interaction kernel in Fourier space $\gamma_2(\vec{k})$ is provided in the Supplemental Material [52]. Interestingly, this function displays the underlying crystalline symmetries as shown in Fig. 1(a), which displacement correlations at linear order do not [47]. Finally, grouping terms and dividing by 2 to avoid double counting of bonds, the excess energy of an arbitrary configuration of defects is then

$$\delta E(\{\delta \sigma_i\}) = \frac{1}{2} \left(\gamma_1 \delta \bar{\sigma}(0) + \sum_{\vec{k}} \gamma_2(\vec{k}) \delta \bar{\sigma}(\vec{k}) \delta \bar{\sigma}(-\vec{k}) \right). \quad (8)$$

We note that this expression provides the exact energy of a disordered configuration, given the incremental sizes $\{\delta \sigma_i\}$ of the particles.

Disorder-averaged defect interactions. We next use our formalism to compute the energy of interaction between defects in a disordered background arising from polydispersity in particle sizes. We consider two particles with larger radii $\delta \sigma_1$

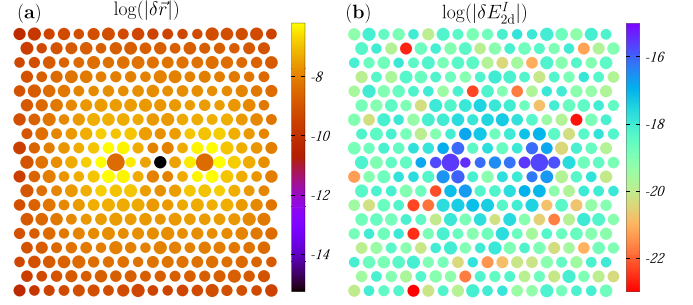


FIG. 2. Section of an energy-minimized configuration of a disordered jammed crystal with two defects. Disorder is introduced into the particle radii (with initial values $\sigma_i^{(0)} = 1/2$), with a polydispersity scale $\eta = 5 \times 10^{-6}$. The defect particles have an excess size 5×10^{-3} . (a) Displacements $\delta \vec{r}$ from the crystalline positions are localized near the defects. (b) Excess interaction energy δE_{2d}^I between the defects is more heterogeneously distributed.

and $\delta \sigma_2$ in excess of the polydispersity scale, placed a relative distance $\vec{\Delta}$ apart. We place the defects at positions $\vec{0} = (0, 0)$ and $\vec{\Delta} = (\Delta_x, \Delta_y)$; therefore $\delta \bar{\sigma}(\vec{k}) = \sum_{\vec{r}} \delta \sigma(\vec{r}) \exp(i\vec{k} \cdot \vec{r}) = \delta \sigma_1 + \delta \sigma_2 \exp(i\vec{k} \cdot \vec{\Delta})$. The energy of the system for the configuration with two defects can be expressed as $E = E^{(0)} + \delta E_{1d}(\vec{0}) + \delta E_{1d}(\vec{\Delta}) + \delta E_{2d}^I(\vec{0}, \vec{\Delta})$, where each of the terms depends on the quenched disorder arising from the polydispersity $\{\delta \sigma_i\}$. Here $\delta E_{1d}(\vec{0})$ and $\delta E_{1d}(\vec{\Delta})$ represent the excess energy associated with the defects 1 and 2 placed in the quenched background, respectively, and $\delta E_{2d}^I(\vec{0}, \vec{\Delta})$ represents the energy of interaction between the defects in the presence of the quenched disorder. We therefore have

$$\delta E_{2d}^I(\vec{0}, \vec{\Delta}) = \delta E_{2d}(\vec{0}, \vec{\Delta}) - \delta E_{1d}(\vec{0}) - \delta E_{1d}(\vec{\Delta}). \quad (9)$$

The displacement fields as well as the interaction energy of a disordered configuration with two defects using the expression (9) are plotted in Fig. 2. For large distances between defects ($|\vec{\Delta}| \rightarrow \infty$), $\delta E_{2d}(\vec{0}, \vec{\Delta}) \rightarrow 0$, and the total energy of the system can be expressed as $E_\infty = E^{(0)} + \delta E_{1d}(\vec{0}) + \delta E_{1d}(\vec{\Delta})$. Therefore, the energy of interaction between two defects can be obtained as $\delta E_{2d}^I(\vec{0}, \vec{\Delta}) = E - E_\infty$. As E_∞ is not accessible for finite system sizes, we consider the largest possible separation between defects. When the two defects are at a relative separation $\vec{\Delta}$, we choose $E_\infty \equiv E_{\vec{L}_{\max}}$, where \vec{L}_{\max} represents the largest distance along $\vec{\Delta}$. The energy of interaction then takes the form $\delta E_{2d}^I(\vec{\Delta}) = E_{\vec{\Delta}} - E_{\vec{L}_{\max}}$. This energy of interaction fluctuates for different realizations of the underlying disorder in particle sizes. Crucially, the fluctuations of δE_{2d}^I in Eq. (8) are symmetric about the mean (see the Supplemental Material [52] for details), leading to $\langle \delta E_{2d}^I \rangle = \delta E_{2d}^I(\eta = 0)$, where $\langle \rangle$ represents the disorder average over realizations and $\delta E_{2d}^I(\eta = 0)$ represents the energy of the two defects in the crystalline background. Using Eqs. (8) and (9) (see the Supplemental Material [52]), the average energy of interaction for a finite system can be expressed as

$$\langle \delta E_{2d}^I(\vec{0}, \vec{\Delta}) \rangle = \delta \sigma_1 \delta \sigma_2 \sum_{\vec{k}} \gamma_2(\vec{k}) [\cos(\vec{k} \cdot \vec{\Delta}) - \cos(\vec{k} \cdot \vec{L}_{\max})]. \quad (10)$$

The presence of the $\delta\sigma_1\delta\sigma_2$ term in this expression implies that the defects display both positive and negative interaction energies, depending on the positive or negative incremental sizes of the defects. Additionally, as the interaction kernel $\gamma_2(\vec{k})$ possesses the crystalline symmetries, the average interaction energy also displays the sixfold symmetry of the underlying crystalline background, with positive and negative interactions along the lattice and off-lattice angles, respectively. We plot the disorder-averaged interaction energy for arbitrary separations $\vec{\Delta} = (X, Y)$ in Fig. 1(b). Studies of induced dipole interactions in continuum elasticity have also revealed such an angular dependence of the interaction energy [21]. However, our results demonstrate that these interactions also emerge upon disorder average, with individual configurations displaying large heterogeneity, which we characterize below.

We next extract the asymptotic behavior of the average interaction energy at large defect separations. We consider the infinite-system-size limit where the summation in (10) can be converted to an integral. The average energy of interaction between two defects can then be expressed as

$$\langle \delta E_{2d}^I \rangle = \frac{\delta\sigma_1\delta\sigma_2}{4\pi^2} \int_{-\pi}^{\pi} \int_{-\pi}^{\pi} \gamma_2(\vec{k}) \cos(\vec{k} \cdot \vec{\Delta}) dk_x dk_y. \quad (11)$$

The evaluation of this integral is rather involved and we provide the derivation in the Supplemental Material [52]. We focus on defects separated in the x direction, and the final form of the interaction energy in the large-distance limit ($\Delta \rightarrow \infty$) is given by

$$\langle \delta E_{2d}^I \rangle \simeq C \frac{\delta\sigma_1\delta\sigma_2}{\Delta^4}, \quad C = \frac{24\sqrt{3}(1-2\epsilon)^2(\epsilon-1)}{\pi(3-4\epsilon)^2}. \quad (12)$$

Here $\epsilon = 1 - R_0$, where R_0 represents the separation between particles in the initial triangular arrangement with $R_0 = \sqrt{\phi_c}/\phi$. In Fig. 3 we plot the numerically obtained interaction energies between two defects placed in the x direction for $\phi = 0.92$. We find that the average interaction predicted by our theory emerges as more realizations of the disorder are considered. We also demonstrate the convergence of the average interaction energy at large separations to the asymptotic power-law behavior predicted in Eq. (12).

Fluctuations in interaction energy. Finally, we turn our attention to the fluctuations in the interaction energy between defects, which can be used to characterize the emergence of the power-law interaction at large separations. Using the expressions (9) and (10), the variance of the energy of interaction for an infinite system with two defects placed at a distance $\vec{\Delta}$ is given by (see the Supplemental Material [52] for details)

$$\begin{aligned} \langle (\delta E_{2d}^I - \langle \delta E_{2d}^I \rangle)^2 \rangle &= \frac{V\eta^2}{48} \sum_{\vec{k}} \gamma_2(\vec{k})\gamma_2(-\vec{k}) \\ &\times [\delta\sigma_1^2 + \delta\sigma_2^2 + \delta\sigma_1\delta\sigma_2 \cos(\vec{k} \cdot \vec{\Delta})]. \end{aligned} \quad (13)$$

Interestingly, this variance in the interaction energy differs from the variance of the excess energies of the individual defects, as it depends on the distance $\vec{\Delta}$. This implies that the fluctuations in the interaction energy produced by two

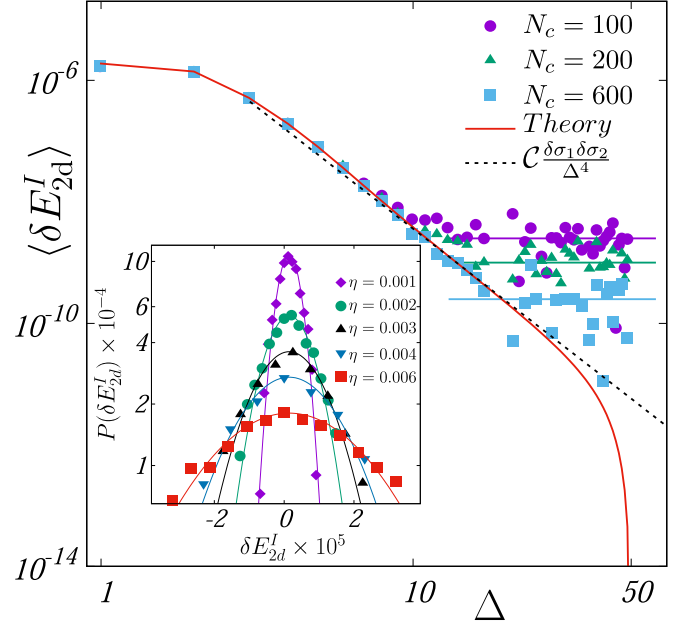


FIG. 3. Average interaction energy between two defects in a disordered background. The points represent data from simulations, while the solid red line represents our theoretical prediction for the interaction energy in Eq. (10). The numerically obtained energy converges to the theoretical prediction with an increasing number of configurations N_c . The average energy displays an asymptotic Δ^{-4} behavior at large separations. The inset shows the distribution of interaction energy between two defects placed at a distance of two lattice spacings apart for five different polydispersities. This energy is Gaussian distributed and matches our predictions for the mean and variance in Eqs. (10) and (14) exactly. Here we choose $\delta\sigma_1 = \delta\sigma_2 = 5 \times 10^{-3}$ and $\phi = 0.92$.

defects encodes the correlations produced by the microscopic disorder. In the inset of Fig. 3 we plot the distributions of the interaction energy along with the above theoretical predictions for five different η , displaying a near-exact match. The theoretical framework developed above is exact in the limit when no contacts are broken in the system. However, even at higher polydispersity with a small number of broken contacts, our predictions yield accurate results. Since contact breaking events affect the local elasticity properties in their neighborhood, deviations from our exact predictions are expected as a large number of contacts break in the system (see the Supplemental Material for details [52]).

Discussion. In this Letter we have presented exact results for the fluctuations in energy of near-crystalline athermal systems. This was enabled by an exact characterization of the displacement fields for small disorder, which satisfies the microscopic force balance constraints. We used this framework to derive the average energy of interaction between defects in the presence of quenched disorder in particle sizes. Remarkably, the nontrivial power-law decay with distance approximately equal to Δ^{-4} of continuum elasticity is recovered in this limit [21,38]. Our results represent a microscopic derivation of this induced dipole effect in a disordered background. Moreover, our formulation allows us to predict the fluctuations in the energy of interaction, which matches our

numerical results from energy-minimized configurations of disordered athermal crystals exactly. The average energy of interaction displays an interesting angular dependence that encodes the symmetries of the underlying crystalline background. Our theoretical framework is exact in the regime of small polydispersity, where all contacts are intact, and the system can be treated as a disordered spring network. However, with increasing polydispersity, contacts between particles are lost. Nevertheless, with a few broken contacts in the system, the large-scale elasticity properties of the network are unaffected and our predictions match well with data from simulations (see Fig. S3 in the Supplemental Material [52]). At large polydispersity, the model under consideration displays a transition to an amorphous state, with large heterogeneity in the contact numbers of particles [28]. Additionally, for very large disorder, decreasing the packing fraction can lead

to unjamming, where the contact network is isostatic. Such situations do not possess the symmetries of the crystalline state and therefore are not captured within the perturbative framework developed in this study. It would be interesting to analyze the effects of larger disorder in the system, in order to understand how rotational symmetry is recovered in the amorphous state, the nature of which continues to be the subject of intense scrutiny.

Acknowledgments. We thank P. Chaudhuri, S. Henkes, B. Chakraborty, S. Bhattacharjee, J. Nampoothiri, V. V. Krishnan, R. Maharana, N. Rana, and V. Pandey for useful discussions. We acknowledge the contributions of S. Sengupta, now sadly deceased, to the initial part of this work. This project was funded by intramural funds at TIFR Hyderabad from the Department of Atomic Energy, Government of India.

-
- [1] M. E. Cates, J. P. Wittmer, J.-P. Bouchaud, and P. Claudin, *Phys. Rev. Lett.* **81**, 1841 (1998).
- [2] C. S. O'Hern, L. E. Silbert, A. J. Liu, and S. R. Nagel, *Phys. Rev. E* **68**, 011306 (2003).
- [3] M. Wyart, *Ann. Phys. Fr.* **30**, 1 (2005).
- [4] K. Ramola and B. Chakraborty, *Phys. Rev. Lett.* **118**, 138001 (2017).
- [5] A. Boromand, A. Signoriello, F. Ye, C. S. O'Hern, and M. D. Shattuck, *Phys. Rev. Lett.* **121**, 248003 (2018).
- [6] C. P. Broedersz, X. Mao, T. C. Lubensky, and F. C. MacKintosh, *Nat. Phys.* **7**, 983 (2011).
- [7] D. Bi, X. Yang, M. C. Marchetti, and M. L. Manning, *Phys. Rev. X* **6**, 021011 (2016).
- [8] L. Berthier and G. Biroli, *Rev. Mod. Phys.* **83**, 587 (2011).
- [9] A. Baule, F. Morone, H. J. Herrmann, and H. A. Makse, *Rev. Mod. Phys.* **90**, 015006 (2018).
- [10] S. Henkes, C. S. O'Hern, and B. Chakraborty, *Phys. Rev. Lett.* **99**, 038002 (2007).
- [11] D. Bi, S. Henkes, K. E. Daniels, and B. Chakraborty, *Annu. Rev. Condens. Matter Phys.* **6**, 63 (2015).
- [12] L. D. Landau and E. M. Lifshitz, *Fluid Mechanics* (Pergamon, Oxford, 1987).
- [13] B. Cui, G. Ruocco, and A. Zaccone, *Granul. Matter* **21**, 1 (2019).
- [14] G. Biroli and P. Urbani, *Nat. Phys.* **12**, 1130 (2016).
- [15] J. N. Nampoothiri, Y. Wang, K. Ramola, J. Zhang, S. Bhattacharjee, and B. Chakraborty, *Phys. Rev. Lett.* **125**, 118002 (2020).
- [16] E. DeGiuli, *Phys. Rev. Lett.* **121**, 118001 (2018).
- [17] A. Lemaître, C. Mondal, I. Procaccia, and S. Roy, *Phys. Rev. B* **103**, 054110 (2021).
- [18] A. Lemaître, *Phys. Rev. Lett.* **113**, 245702 (2014).
- [19] H. Askari and K. Kamrin, *Nat. Mater.* **15**, 1274 (2016).
- [20] J. H. Snoeijer, T. J. H. Vlugt, M. van Hecke, and W. van Saarloos, *Phys. Rev. Lett.* **92**, 054302 (2004).
- [21] P. Peyla, A. Vallat, C. Misbah, and H. Müller-Krumbhaar, *Phys. Rev. Lett.* **82**, 787 (1999).
- [22] O. Gendelman, E. Lerner, Y. G. Pollack, I. Procaccia, C. Rainone, and B. Riechers, *Phys. Rev. E* **94**, 051001(R) (2016).
- [23] J. P. Steimel, J. L. Aragones, H. Hu, N. Qureshi, and A. Alexander-Katz, *Proc. Natl. Acad. Sci. USA* **113**, 4652 (2016).
- [24] L. Bereziani and J. Khoury, *Phys. Rev. D* **99**, 076003 (2019).
- [25] T. Qian, X.-P. Wang, and P. Sheng, *Solid State Commun.* **150**, 976 (2010).
- [26] M. Puljiz, S. Huang, G. K. Auernhammer, and A. M. Menzel, *Phys. Rev. Lett.* **117**, 238003 (2016).
- [27] C. P. Goodrich, A. J. Liu, and S. R. Nagel, *Nat. Phys.* **10**, 578 (2014).
- [28] H. Tong, P. Tan, and N. Xu, *Sci. Rep.* **5**, 15378 (2015).
- [29] P. Acharya, D. Das, and K. Ramola, *Phys. Rev. E* **104**, 034608 (2021).
- [30] G. Tsekenis, *Europhys. Lett.* **135**, 36001 (2021).
- [31] P. Charbonneau, E. I. Corwin, L. Fu, G. Tsekenis, and M. van der Naald, *Phys. Rev. E* **99**, 020901(R) (2019).
- [32] H. Mizuno, S. Mossa, and J.-L. Barrat, *Europhys. Lett.* **104**, 56001 (2013).
- [33] M. Kellomäki, J. Åström, and J. Timonen, *Phys. Rev. Lett.* **77**, 2730 (1996).
- [34] M. Ostoja-Starzewski, *Appl. Mech. Rev.* **55**, 35 (2002).
- [35] K. Lau and W. Kohn, *Surf. Sci.* **65**, 607 (1977).
- [36] J. Eshelby, in *Solid State Physics*, edited by F. Seitz and D. Turnbull (Elsevier, Amsterdam, 1956), Vol. 3, pp. 79–144.
- [37] O. L. Alerhand, D. Vanderbilt, R. D. Meade, and J. D. Joannopoulos, *Phys. Rev. Lett.* **61**, 1973 (1988).
- [38] P. Peyla and C. Misbah, *Eur. Phys. J. B* **33**, 233 (2003).
- [39] V. Marchenko and C. Misbah, *Eur. Phys. J. E* **8**, 477 (2002).
- [40] R. Golkov and Y. Shokef, *Phys. Rev. E* **99**, 032418 (2019).
- [41] X. Zhang, K. Jiao, P. Sharma, and B. Yakobson, *J. Mech. Phys. Solids* **54**, 2304 (2006).
- [42] R. Golestanian, M. Goulian, and M. Kardar, *Phys. Rev. E* **54**, 6725 (1996).
- [43] R. Golestanian, M. Goulian, and M. Kardar, *Europhys. Lett.* **33**, 241 (1996).
- [44] M. Goulian, R. Bruinsma, and P. Pincus, *Europhys. Lett.* **22**, 145 (1993).
- [45] C. Sirote and Y. Shokef, *Phys. Rev. E* **104**, 024411 (2021).
- [46] P. Acharya, S. Sengupta, B. Chakraborty, and K. Ramola, *Phys. Rev. Lett.* **124**, 168004 (2020).

- [47] D. Das, P. Acharya, and K. Ramola, *Phys. Rev. E* **104**, 014503 (2021).
- [48] D. Das, P. Acharya, and K. Ramola, *J. Stat. Phys.* **189**, 26 (2022).
- [49] R. Maharana, J. N. Nampoothiri, and K. Ramola, [arXiv:2202.04094](https://arxiv.org/abs/2202.04094).
- [50] D. J. Durian, *Phys. Rev. Lett.* **75**, 4780 (1995).
- [51] C. S. O'Hern, S. A. Langer, A. J. Liu, and S. R. Nagel, *Phys. Rev. Lett.* **88**, 075507 (2002).
- [52] See Supplemental Material at <http://link.aps.org/supplemental/10.1103/PhysRevE.106.L052902> for details.
- [53] E. Bitzek, P. Koskinen, F. Gähler, M. Moseler, and P. Gumbsch, *Phys. Rev. Lett.* **97**, 170201 (2006).
- [54] T. Horiguchi, *J. Math. Phys.* **13**, 1411 (1972).